



The hadronic τ decay $\tau^- \rightarrow K_1^- \nu_\tau \rightarrow (K^- \omega) \nu_\tau \rightarrow (K^- \pi^+ \pi^- \pi^0) \nu_\tau$ and the axial vector mixing angle

K. Hayasaka¹, Z. Huang², E. Kou^{2,a}

¹ Niigata University, 8050 Ikarashi 2-no-cho, Nishi-ku, Niigata 950-2181, Japan

² Université Paris-Saclay, CNRS/IN2P3, IJCLab, 91405 Orsay, France

Received: 7 April 2021 / Accepted: 30 May 2021

© The Author(s) 2021

Abstract We propose to measure the $\tau^- \rightarrow K_1^- \nu_\tau \rightarrow (K^- \omega) \nu_\tau \rightarrow (K^- \pi^+ \pi^- \pi^0) \nu_\tau$ decay in order to determine the K_1 axial vector mixing angle θ_{K_1} . We derive, for the first time, the differential decay rate formula for this decay mode. Using the obtained result, we perform a sensitivity study for the Belle (II) experiment. We will show that the $K^- \pi^+ \pi^- \pi^0$ spectrum of the $\tau^- \rightarrow K_1^- \nu_\tau \rightarrow (K^- \omega) \nu_\tau \rightarrow (K^- \pi^+ \pi^- \pi^0) \nu_\tau$ decay can discriminate the two solutions $\theta_{K_1} \approx 30^\circ$ or $\sim 60^\circ$ observed in the other measurements.

1 Introduction

The hadronic τ decay is a very useful tool to investigate the nature of the light hadrons. The initial state being lepton allows to study the strong decays of the final state hadrons in a clean manner. The hadrons being produced from the W boson provides a valuable information on the vector and the axial vector couplings of the hadrons. In this article, we investigate the $\Delta S = 1$ hadronic τ decay. This type of decays is Cabibbo suppressed but offers unique way to explore the nature of the Kaonic resonances [1]. We investigate the $\tau^- \rightarrow K_1^- \nu_\tau \rightarrow (K^- \omega) \nu_\tau \rightarrow (K^- \pi^+ \pi^- \pi^0) \nu_\tau$ decay to obtain the information of the K_1 axial vector mesons, $K_1(1270)$ and $K_1(1400)$. A better understanding of the K_1 mesons is not only an interest of its own but also is highly demanded by B physics recently. In B physics, to disentangle the new physics effect from the hadronic uncertainties is the essential task for a discovery. The recent studies of $B \rightarrow K_1 \gamma$ decays [2–6], $B \rightarrow K_1 \ell^+ \ell^-$ [7] or $B \rightarrow K_1 \pi$ decays [8–10], which are known to be sensitive to the new physics coming from the right-handed current or the CP violation, respectively, show that a more accurate information of the K_1 mesons would enhance the sensitivity to the new physics.

In this article, we propose to measure the $\tau^- \rightarrow K_1^- \nu_\tau \rightarrow (K^- \omega) \nu_\tau \rightarrow (K^- \pi^+ \pi^- \pi^0) \nu_\tau$ decay to determine the θ_{K_1} angle. The θ_{K_1} enters both in the production and the decay of K_1 meson in this process. The determination of the axial-vector mixing angle caused a controversy. Mainly two ways to determine θ_{K_1} have been attempted, (i) mass fit assuming the $SU(3)$, (ii) strong decay of K_1 . Both show basically two possible solutions far apart, around $\sim 30^\circ$ and $\sim 60^\circ$ (see e.g. [11–16]). In this article, we show the result of the 5 body differential decay rate, $\tau^- \rightarrow K_1^- \nu_\tau \rightarrow (K^- \omega) \nu_\tau \rightarrow (K^- \pi^+ \pi^- \pi^0) \nu_\tau$, for the first time. Then, we use this result to perform a sensitivity study for θ_{K_1} determination at the Belle II experiment. This process was studied in ALEPH [17, 18] and CLEO [19] experiments and a few hundreds of events are observed. The Belle II experiment can acquire 2–3 orders of magnitudes more data in the future.

The remaining of the article is organised as follows. In Sect. 2, we derive the 5 body differential decay rate. In Sect. 3, we introduce the mixing angle and rewrite our results in terms of θ_{K_1} . We show our numerical result and the Monte Carlo study assuming the Belle (II) setup in Sect. 4 and we conclude in Sect. 5.

2 Differential decay rate of $\tau^- \rightarrow K_1^- \nu_\tau \rightarrow (K^- \omega) \nu_\tau \rightarrow (K^- \pi^+ \pi^- \pi^0) \nu_\tau$

We first present the computation for the decay rate of the five body decay (4 momentum associated to each particle is given in the parenthesis)

$$\begin{aligned} \tau^-(Q) &\rightarrow K_1^-(k_1) \nu_\tau(p_0) \rightarrow K^-(p_1) \omega(k_2) \nu_\tau(p_0) \\ &\rightarrow K^-(p_1) \pi^+(p_2) \pi^-(p_3) \pi^0(p_4) \nu_\tau(p_0) \end{aligned} \quad (1)$$

^a e-mail: kou@lal.in2p3.fr (corresponding author)

where K_1 is a $J^P = 1^+$ meson, i.e. $K_1(1270)$ or $K_1(1400)$. The five body differential decay rate can be given as

$$d\Gamma = \frac{(2\pi)^4}{2m_\tau} |\mathcal{M}|^2 d\Phi_5 \quad (2)$$

where

$$d\Phi_5 = \frac{1}{(2\pi)^{14}} \frac{1}{\left(2^7 m_\tau \sqrt{k_2^2}\right)} |\vec{p}_1| |\vec{p}_0| d\sqrt{k_2^2} d \\ \times \sqrt{k_1^2} dm_{23}^2 dm_{34}^2 d(\cos\theta) d\bar{\phi} d\bar{\psi} d\bar{\Omega} d\Omega. \quad (3)$$

The variables with $\vec{}$ and $\bar{}$ are the momentum and polar angles in the rest frame of K_1 and ω , respectively. Since the angular dependence is not easy to measure in τ decays, we integrate them all in this work. Thus, the remaining integration variables are the invariant masses of K_1, ω and two Dalitz variables of ω decays, which are given as

$$k_1^2 = (p_1 + p_2 + p_3 + p_4)^2, \quad k_2^2 = (p_2 + p_3 + p_4)^2, \\ m_{23}^2 = (p_2 + p_3)^2, \quad m_{34}^2 = (p_3 + p_4)^2. \quad (4)$$

The 3-momentum of $\nu_\tau, |\vec{p}_0|$, and of the final state $K, |\vec{p}_1|$, are written by the integration variables, $\sqrt{k_2^2}$ and $\sqrt{k_1^2}$, as

$$|\vec{p}_0| = \frac{m_\tau^2 - k_1^2}{2m_\tau} \quad (5)$$

$$|\vec{p}_1| = \frac{\sqrt{\left(k_1^2 - \left(m_1 + \sqrt{k_2^2}\right)^2\right) \left(k_1^2 - \left(m_1 - \sqrt{k_2^2}\right)^2\right)}}{2\sqrt{k_1^2}}. \quad (6)$$

The decay amplitude \mathcal{M} is obtained as a product of the successive decay amplitudes, i.e.:

$$\mathcal{M} = \mathcal{M}_3(\omega \rightarrow \pi^+ \pi^- \pi^0) \times \mathcal{M}_2(K_1^- \rightarrow K^- \omega) \\ \times \mathcal{M}_1(\tau^- \rightarrow K_1^- \nu_\tau). \quad (7)$$

The amplitude of the $\tau \rightarrow K_1 \nu_\tau$ can be written as

$$\mathcal{M}_1(\tau \rightarrow K_1 \nu_\tau) = \frac{G_F}{m_\tau} V_{us}^* j_\mu \langle K_1 | \bar{s} \gamma^\mu (1 - \gamma_5) u | 0 \rangle \quad (8)$$

where the leptonic current is given as

$$j_\mu = \bar{\nu}_\tau \gamma_\mu (1 - \gamma_5) \tau. \quad (9)$$

The K_1 meson can be produced only from the axial vector current and the matrix element of K_1 production is given by a decay constant f_{K_1}

$$\langle K_1 | \bar{s} \gamma^\mu (1 - \gamma_5) u | 0 \rangle = -i f_{K_1} m_{K_1} \epsilon^{*\mu}(k_1) \quad (10)$$

where K_1 is only symbolic here and it can mean $K_1(1270)$ or $K_1(1400)$. The detailed definitions of the decay constants for these two states are given in the next section.

The amplitude of the $K_1 \rightarrow K \omega$ decay can be written by the two form factors

$$\mathcal{M}_2(K_1 \rightarrow K \omega) = \epsilon_{K_1}^\mu T_{\mu\nu} \epsilon_\omega^{*\nu} \quad (11)$$

where

$$T_{\mu\nu} = f^{K_1} g_{\mu\nu} + h^{K_1} k_{2\mu} p_{1\nu}. \quad (12)$$

Note that these form factors can be related to the S-wave and P-wave amplitudes (see Appendix D of [20] for derivation)

$$f^{K_1} = -A_S^{K_1} - \frac{1}{\sqrt{2}} A_D^{K_1} \quad (13)$$

$$h^{K_1} = \frac{\tilde{E}_\omega}{\sqrt{k_1^2} |\vec{p}_1|^2} \left[\left(1 - \frac{\sqrt{k_2^2}}{\tilde{E}_\omega}\right) A_S^{K_1} + \left(1 + \frac{2\sqrt{k_2^2}}{\tilde{E}_\omega}\right) \frac{1}{\sqrt{2}} A_D^{K_1} \right] \quad (14)$$

where $\tilde{E}_\omega = \sqrt{|\vec{p}_1|^2 + k_2^2}$. As the decay rates of S-wave and D-wave are not separately known, we must rely on the theoretical model as we will see late-on.

The amplitude of the $\omega \rightarrow \pi^+ \pi^- \pi^0$ can be written by one form factor

$$\mathcal{M}_3(\omega \rightarrow \pi^+ \pi^- \pi^0) = i g \epsilon_{\mu\nu\alpha\beta} \epsilon^\mu p_2^\nu p_3^\alpha p_4^\beta \mathcal{F} \quad (15)$$

where assuming that the $\omega \rightarrow 3\pi$ go through three possible resonances, ρ^+, ρ^- and ρ^0 , we can simply write the form factor to be

$$\mathcal{F} = \frac{1}{m_{24}^2 - m_{\rho^+}^2 + i m_{\rho^+} \Gamma_{\rho^+}} + \frac{1}{m_{34}^2 - m_{\rho^-}^2 + i m_{\rho^-} \Gamma_{\rho^-}} \\ + \frac{1}{m_{23}^2 - m_{\rho^0}^2 + i m_{\rho^0} \Gamma_{\rho^0}} \quad (16)$$

where we assign $p_{2,3,4}$ as the 4-momentum of π^+, π^-, π^0 .

Finally, the squared amplitudes after integration of all the angles is obtained as¹

$$d\Gamma(\tau \rightarrow K_1 \nu \rightarrow K \omega \nu \rightarrow K \pi \pi \nu) \\ \frac{d\sqrt{k_1^2} d\sqrt{k_2^2} dm_{23}^2 dm_{34}^2}{(2\pi)^{10}} |\vec{p}_1| |\vec{p}_0| \quad (17)$$

$$|\mathcal{M}|^2 = \left(\frac{G_F V_{us} m_{K_1} g}{m_\tau}\right)^2 |\mathcal{F}|^2 \\ \times \frac{512\pi^4}{27k_1^2} m_\tau |\vec{p}_0| |\vec{p}_2|^2 |\vec{p}_3|^2 \sin^2 \delta \left(4m_\tau^2 + 12k_1^2 + \frac{2k_1^4}{m_\tau^2}\right) C \quad (18)$$

¹ As we integrate all the angles, all the spins can be summed after squaring the amplitude.

where

$$\delta = \cos^{-1} \left[\frac{E_{\pi^+} E_{\pi^-} + \frac{2m_{\pi^+}^2 - m_{\pi^-}^2}{2}}{\sqrt{E_{\pi^+}^2 - m_{\pi^+}^2} \sqrt{E_{\pi^-}^2 - m_{\pi^-}^2}} \right].$$

The factor \mathcal{C} is

$$\mathcal{C} = (2|F_0|^2 + |F_1|^2)$$

with

$$F_0 = f_{K_1} f^{K_1} \mathcal{B}\mathcal{W}_{K_1} \tag{19}$$

$$F_1 = \left[f_{K_1} \left(f^{K_1} \tilde{E}_{\omega} + h^{K_1} \sqrt{k_1^2} |\tilde{p}_1|^2 \right) \mathcal{B}\mathcal{W}_{K_1} \right] / \sqrt{k_2^2} \tag{20}$$

and

$$\mathcal{B}\mathcal{W}_{K_1} = \frac{1}{k_1^2 - m_{K_1}^2 + im_{K_1} \Gamma_{K_1}}.$$

As we are interested in the contributions from $K_1(1270)$ and $K_1(1400)$ as well as their interference, we sum them at the amplitude level and take a square. Further replacing the form factors to the partial wave amplitudes, we obtain the \mathcal{C} function as

$$\begin{aligned} \mathcal{C} = 3 \left\{ \right. & \left| f_{K_1(1270)} A_S^{K_1(1270)} \mathcal{B}\mathcal{W}_{K_1(1270)} \right. \\ & \left. + f_{K_1(1400)} A_S^{K_1(1400)} \mathcal{B}\mathcal{W}_{K_1(1400)} \right|^2 \\ & \left. + \left| f_{K_1(1270)} A_D^{K_1(1270)} \mathcal{B}\mathcal{W}_{K_1(1270)} \right. \right. \\ & \left. \left. + f_{K_1(1400)} A_D^{K_1(1400)} \mathcal{B}\mathcal{W}_{K_1(1400)} \right|^2 \right\}. \tag{21} \end{aligned}$$

In the next section, we obtain the decay constants $f_{K_1(1270,1400)}$ as well as the partial wave amplitudes $A_{S,D}^{K_1(1270,1300)}$ in terms of the axial vector mixing angle θ_{K_1} .

3 The axial vector mixing angle θ_{K_1}

The axial vector strange mesons have a peculiar nature, the observed physical states, $K_1(1270)$ and $K_1(1400)$ are the mixture of two $J^P = 1^+$ states, 3P_1 and 1P_1 . This is different from the case of the non-strange axial vector mesons, $a_1(1260)$ and $b_1(1235)$, which do not mix as the 3P_1 and 1P_1 states are also the eigenstates of different intrinsic charge, i.e. ($J^{PC} = 1^{++}, 1^{+-}$). Let us denote the unphysical 3P_1 and 1P_1 states as K_{1a} and K_{1b} , respectively. Then, the physical states (mass eigenstates) can be written as

$$\begin{pmatrix} K_1(1270) \\ K_1(1400) \end{pmatrix} = \begin{pmatrix} \sin \theta_{K_1} & \cos \theta_{K_1} \\ \cos \theta_{K_1} & -\sin \theta_{K_1} \end{pmatrix} \begin{pmatrix} K_{1a} \\ K_{1b} \end{pmatrix} \tag{22}$$

where θ_{K_1} is called as the axial vector mixing angle.

Investigating the nature of the strange axial vector mesons produced from τ decay, i.e. the weak interaction, has a great

advantage. The spin singlet configuration of the s and u quarks are suppressed with respect to the spin triplet one as the former is chirally forbidden and furthermore, the $SU(3)$ and charge symmetry forbids the production of K_{1b} [21]. This leads to, at the first order, that only the K_{1a} is produced from the weak interaction. Therefore, by defining the decay constant of K_{1a}, K_{1b} state,

$$\langle K_{1a,1b} | \bar{s} \gamma^{\mu} (1 - \gamma_5) u | 0 \rangle = -i f_{K_{1a,1b}} m_{K_{1a,1b}} \epsilon^{*\mu}(k_1), \tag{23}$$

we have $f_{K_{1a}} \gg f_{K_{1b}} \simeq 0$. Then, by using Eq. (22), the decay constant of the physical states can be given as

$$f_{K_1(1270)} = f_{K_{1a}} \sin \theta_{K_1}, \quad f_{K_1(1400)} = f_{K_{1a}} \cos \theta_{K_1}. \tag{24}$$

Since the s quark mass is not completely negligible with respect to the K_1 masses, $f_{K_{1b}}$ may not vanish. This effect can be taken into account by shifting the mixing angle by $\delta_s = \tan^{-1} \left(\frac{f_{K_{1b}}}{f_{K_{1a}}} \right)$,

$$f_{K_1(1270)} = f_{K_{1a}} \sin \theta'_{K_1}, \quad f_{K_1(1400)} = f_{K_{1a}} \cos \theta'_{K_1} \tag{25}$$

where $\theta'_{K_1} \equiv \theta_{K_1} + \delta_s$. We investigate maximum of 10% of s quark mass effect, i.e. $|\delta_s| < 0.1$ (6°), in the following.

Next, we consider the strong decay, $K_1 \rightarrow K\omega$. We use the result of the quark model computation in [14], where a similar process, $K_1 \rightarrow K\rho$ decay, is investigated. Using the $SU(3)$ symmetry, the S -wave and D -wave amplitudes for the K_{1a} and K_{1b} states can be written by the universal amplitudes, S^{ABC} and D^{ABC} as (see [14] for derivation)

$$\begin{aligned} A_S^{K_{1a}} &= \sqrt{\frac{2}{3}} S^{ABC}, & A_D^{K_{1a}} &= -\frac{1}{\sqrt{3}} D^{ABC}, \\ A_S^{K_{1b}} &= \frac{1}{\sqrt{3}} S^{ABC}, & A_D^{K_{1b}} &= \sqrt{\frac{2}{3}} D^{ABC}. \end{aligned} \tag{26}$$

Then, the amplitudes for the physical states yield

$$\begin{aligned} A_S^{K(1270)} &= A_S^{K_{1a}} \sin \theta_{K_1} + A_S^{K_{1b}} \cos \theta_{K_1} \\ &= S^{ABC} \sin(\theta_{K_1} + \theta_0) \end{aligned} \tag{27}$$

$$\begin{aligned} A_D^{K(1270)} &= A_D^{K_{1a}} \sin \theta_{K_1} + A_D^{K_{1b}} \cos \theta_{K_1} \\ &= D^{ABC} \cos(\theta_{K_1} + \theta_0) \end{aligned} \tag{28}$$

$$\begin{aligned} A_S^{K(1400)} &= A_S^{K_{1a}} \cos \theta_{K_1} - A_S^{K_{1b}} \sin \theta_{K_1} \\ &= -S^{ABC} \cos(\theta_{K_1} + \theta_0) \end{aligned} \tag{29}$$

$$\begin{aligned} A_D^{K(1400)} &= A_D^{K_{1a}} \cos \theta_{K_1} - A_D^{K_{1b}} \sin \theta_{K_1} \\ &= -D^{ABC} \sin(\theta_{K_1} + \theta_0) \end{aligned} \tag{30}$$

where $\theta_0 = \tan^{-1} \frac{1}{\sqrt{2}} \simeq 35.26^\circ$. It is important to mention that we do not expect a $SU(3)$ breaking effect beyond this result. It is because the K_{1a} and K_{1b} mixing occurs via the very hadronic decays, $K_1 \rightarrow K\omega$ as well as $K\rho, K^*\pi$ (i.e. hadronic contributions in the loop). The $SU(3)$ breaking effect, which comes from the mass difference among these

intermediate states, is taken into account via the non-zero θ_{K_1} angle.

Finally, we can simplify Eq. (21) by using the mixing angle as

$$\begin{aligned}
 \mathcal{C} = & 3|f_{K_{1a}}|^2 \left\{ |S^{ABC}|^2 \left| \sin \theta'_{K_1} \sin(\theta_{K_1} + \theta_0) \mathcal{BW}_{K_1(1270)} \right. \right. \\
 & + \left. \left. \cos \theta'_{K_1} \cos(\theta_{K_1} + \theta_0) \mathcal{BW}_{K_1(1400)} \right|^2 \right. \\
 & + |D^{ABC}|^2 \left| \sin \theta'_{K_1} \cos(\theta_{K_1} + \theta_0) \mathcal{BW}_{K_1(1270)} \right. \\
 & \left. \left. + \cos \theta'_{K_1} \sin(\theta_{K_1} + \theta_0) \mathcal{BW}_{K_1(1400)} \right|^2 \right\} \quad (31)
 \end{aligned}$$

which is our final result and will be used in the next section. It should be emphasised that the obtained expression is different from the one proposed in [11], where only the θ_{K_1} dependence on the $\tau \rightarrow K_1 \nu$ decay is taken into account but not on the K_1 decay.

4 The numerical results and Belle (II) sensitivity study

In this section, we present the sensitivity of the Belle II experiment to the θ_{K_1} angle. First, we list up all the parameters we use in our numerical analysis. Note that for now, we list only the central values while we will discuss the uncertainties associated to them later-on:

$$\begin{aligned}
 m_\tau &= 1.777 \text{ GeV}, \quad m_{K_1(1270)} = 1.270 \text{ GeV}, \\
 m_{K_1(1400)} &= 1.400 \text{ GeV} \\
 m_K &= 0.494 \text{ GeV}, \quad m_\pi = 0.135 \text{ GeV}, \quad m_\omega = 0.782 \text{ GeV}, \\
 m_\rho &= 0.775 \text{ GeV} \\
 \Gamma_{K_1(1270)} &= 0.09 \text{ GeV}, \quad \Gamma_{K_1(1400)} = 0.174 \text{ GeV}, \\
 \Gamma_\omega &= 0.00849 \text{ GeV}, \quad \Gamma_\rho = 0.148 \text{ GeV}. \quad (32)
 \end{aligned}$$

Since our goal is not to estimate the total decay rate, the overall factors not listed her, such as $G_F, V_{us}, g, f_{K_1} \dots$ are not necessary in this study. For the universal partial wave amplitude, which we introduced in the previous section, the result from the 3P_0 model yields [14]

$$\begin{aligned}
 S^{ABC} &\propto \left(3 - \alpha |\vec{p}_1|^2 \right) e^{-\beta |\vec{p}_1|^2} e^{-f_2 \left(|\vec{p}_1|^2 - |\vec{p}_1^0|^2 \right)}, \\
 D^{ABC} &\propto \alpha |\vec{p}_1|^2 e^{-\beta |\vec{p}_1|^2} e^{-f_2 \left(|\vec{p}_1|^2 - |\vec{p}_1^0|^2 \right)} \quad (33)
 \end{aligned}$$

where $\alpha = 4.2 \text{ GeV}^{-2}, \beta = 0.52 \text{ GeV}^{-2}$ and $f_2 = 3.0$. The last exponential is the so-called damping factor, which introduces the cut off for the large momentum region. The momentum \vec{p}_1^0 is \vec{p}_1 at the pole masses. For $K_1(1270)$, there is no available phase space at the pole mass, thus, the damping factor can be neglected.

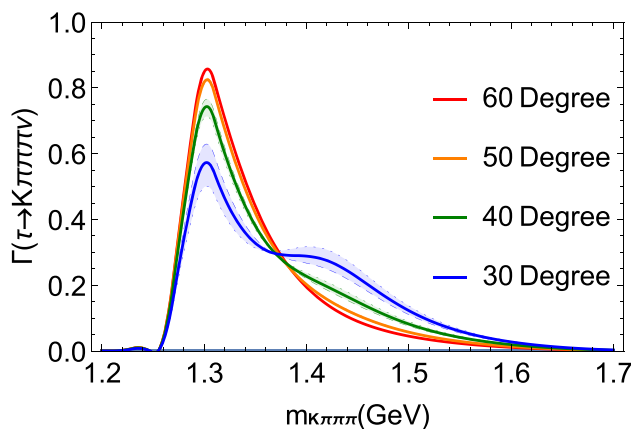


Fig. 1 The $K\pi\pi\pi$ distribution of the $\tau^- \rightarrow K_1^- \nu_\tau \rightarrow (K^- \omega) \nu_\tau \rightarrow (K^- \pi^+ \pi^- \pi^0) \nu_\tau$. The solid line represents the result without the extra $SU(3)$ breaking effect (see text), i.e. $\delta_s = 0$ while the coloured area is with this effect with amount of $|\delta_s| \lesssim 6^\circ$ (the dashed lines are the results for $\delta_s = 6^\circ$ and the dotted lines are for $\delta_s = -6^\circ$)

In order to have an idea of the D -wave contribution, let us quote the mean values of \vec{p}_1 for $K_1(1270)$ and $K_1(1400)$

$$\begin{aligned}
 \langle \vec{p}_1 \rangle_{K_1(1270)} &= (0.19 \pm 0.09) \text{ GeV}, \\
 \langle \vec{p}_1 \rangle_{K_1(1400)} &= (0.28 \pm 0.09) \text{ GeV} \quad (34)
 \end{aligned}$$

where the error comes from the spread of the $\langle \vec{p}_1 \rangle$. This number implies that the D -wave amplitude is roughly 5(10)% for $K_1(1270)(K_1(1400))$ of the S -wave one. As these two contributions do not interfere, we expect the D -wave contributions is very small. In order to simplify the analysis, we use a constant S^{ABC} and D^{ABC} in the present study. So as to take into account the momentum depending term in the S -wave, which is not negligible, we choose different constants for $K_1(1270)$ and $K_1(1400)$. We find the following choices reproduce well the full expression:

$$\begin{aligned}
 S_{K_1(1270)}^{ABC} &= 3.0 \text{ GeV}, \quad D_{K_1(1270)}^{ABC} = 0.2 \text{ GeV}, \\
 S_{K_1(1400)}^{ABC} &= 2.3 \text{ GeV}, \quad D_{K_1(1400)}^{ABC} = 0.3 \text{ GeV} \quad (35)
 \end{aligned}$$

which we will use in our analysis. Later in this section, we discuss the impact of the variations of these parameters.

The $K\pi\pi\pi$ mass distribution (normalised to unity) is shown in Fig. 1. The solid line is the result with no extra $SU(3)$ breaking, mentioned earlier, i.e. $\theta'_{K_1} = \theta_{K_1}$. For the small values of θ_{K_1} , let's say around 30° , the $K\pi\pi\pi$ spectrum changes significantly for a variation of the mixing angle while when the mixing angle reaches around $\sim 50^\circ$, $K_1(1270)$ becomes totally dominant and it becomes difficult to distinguish the results with different θ_{K_1} . This pattern can be readily inferred from the dominant S -wave contributions in Eq. (31). The coefficient for the $K_1(1270)$ contribution, $\sin \theta_{K_1} \sin(\theta_{K_1} + \theta_0)$, is an increasing function in the region of θ_{K_1} we are considering. On the other hand, the coefficient

for $K_1(1400)$, $\cos \theta_{K_1} \cos(\theta_{K_1} + \theta_0)$, rapidly decreases and hits zero at $\theta_{K_1} = 90^\circ - \theta_0 = 54.74^\circ$. The coloured bound in Fig. 1 is results including the extra $SU(3)$ breaking effect with amount of $|\delta_s| \leq 6^\circ$. We can see that this effect has an impact only on the $\sin \theta_{K_1}$ and $\cos \theta_{K_1}$ terms, and as a result, it is almost negligible for $\theta_{K_1} \gtrsim 40^\circ$.

In order to clarify the achievable limit by the Belle (II) experiment, we perform a Monte Carlo study. The $e^+e^- \rightarrow \tau^+\tau^-$ process is simulated by using the KKMC package [22,23] with the Belle beam energy, 8 GeV for electron and 3.5 GeV for positron. We decay the tagging side of τ by using the TAUOLA package [24–26]. We do not consider the spin correlation as we will use only the leptonic decay (e or μ) on the tagging side, which reduces significantly the $q\bar{q}$ background. For the signal side, we use the differential decay rate formulae derived in this article to generate the $\tau^- \rightarrow K_1^- \nu_\tau \rightarrow (K^- \omega) \nu_\tau \rightarrow (K^- \pi^+ \pi^- \pi^0) \nu_\tau$ decay distribution.

The main background comes from $\tau \rightarrow 3\pi\pi^0\nu$ decay, where 3π does not necessarily come from ω but all possible intermediate states, such as $a_1\pi, \rho\rho, \dots$. Thus, we select the four charged tracks with no net charge and evaluate the thrust axis. Here, the ‘good’ charged tracks are defined as $dr < 5$ mm, $|dz| < 5$ cm, $p_t > 100$ MeV and ‘good’ gamma is the one with $E_\gamma > 50$ MeV within the detector fiducial volume. We select the events which have three charged tracks parallel to the thrust axis (signal side) and one anti-parallel (tag side). The signal side should contain two γ with 120 MeV $< M_{\gamma\gamma} < 150$ MeV and $\pi\pi\gamma\gamma$ in the ω mass region, 760 MeV $< M_{\pi\pi\gamma\gamma} < 800$ MeV. We select only those $\gamma\gamma$ in the barrel region to avoid the background. For the simplicity, we ignore the multi-candidate case: if more than two sets of γ satisfy the above condition, we reject such events (the fraction is around a few percents). The charged track which does not construct ω is considered to be kaon. For the detection efficiency computation, we use the Belle detector simulation with the improved kaon identification (ID). That is, we assume kaon ID of Belle II, 90% for kaon ID and 4% for π fake rate for kaon ID [1], which is about twice better than Belle.

We found that the detection efficiency is 1–2%, which results in ~ 10 k event for each ~ 1 ab $^{-1}$ of data. Thus, this amount of data is already available in the Belle experiment. We use 15k event as a benchmark experimental setup in the following analysis.

For the Belle (II) sensitivity study to the axial vector mixing angle θ_{K_1} , we first generate events for different values of θ_{K_1} from 0° to 90° . We use the same input parameters as Fig. 1. The $M_{K\pi\pi\pi}$ spectrum after taking into account the detector effects is given in Fig. 2. The similar spectrums are observed in Figs. 1 and 2, which show that our selection criteria is appropriate.

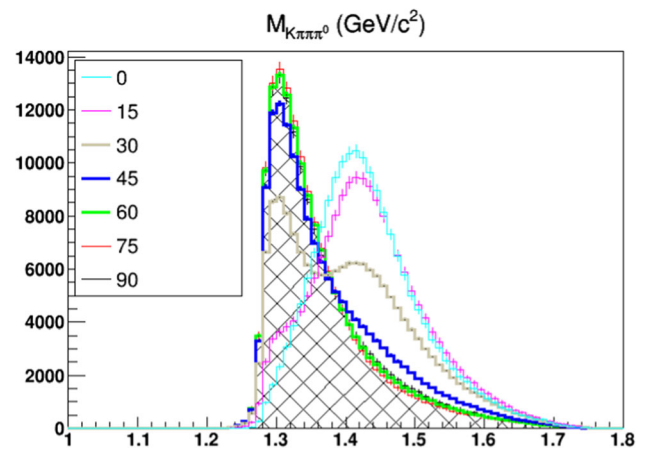


Fig. 2 The $K\pi\pi\pi$ invariant mass distribution of the $\tau^- \rightarrow K_1^- \nu_\tau \rightarrow (K^- \omega) \nu_\tau \rightarrow (K^- \pi^+ \pi^- \pi^0) \nu_\tau$ after taking into account the detector effect of Belle

Next, using the generated events, we fit the θ_{K_1} angle. With the 15k of events, we find the statistical error to be

$$\begin{aligned} \sigma_{(\theta_{K_1}=15^\circ)} &= 0.3^\circ, & \sigma_{(\theta_{K_1}=30^\circ)} &= 0.2^\circ, \\ \sigma_{(\theta_{K_1}=45^\circ)} &= 0.4^\circ, & \sigma_{(\theta_{K_1}=60^\circ)} &= 1.1^\circ, & \sigma_{(\theta_{K_1}=75^\circ)} &= 1.9^\circ. \end{aligned} \tag{36}$$

The very small errors estimated with the amount of data which will be soon available, are very encouraging. Thus, we further investigate the various systematic uncertainties. This is particularly important as the $K\pi\pi\pi$ invariant mass distributions for $\theta_{K_1} \gtrsim 40^\circ$ seem to be very difficult to distinguish and the systematic effect could dominate. To evaluate the experimental systematic error is beyond the scope of this article while we investigate the systematic errors coming from the input parameters in the following.

As mentioned earlier, since our goal is to determine the mixing angle and not the total branching ratio, the overall factors do not induce an uncertainty. The most uncertain input parameters are the mass and width of the $K_1(1270)$ resonance in Eq. (32) as well as the S -wave and D -wave amplitudes in Eq. (35). Both induce the similar kinds of uncertainties in the line shape of the K_1 resonances. To identify the line shape of the K_1 resonance is a long-standing challenge: the dominant decay channel $K_1(1270) \rightarrow \rho K$ has no phase space at the pole mass, which distorts the line shape [27]. This issue is investigated intensively in [14] using the kaon beam experiment data [28]. Our prescription, to take into account the line shape ambiguity, here is that we free the mass and width of $K_1(1270)$ while fitting the θ_{K_1} . We emphasise that this prescription can accommodate not only the mass and width uncertainties but also the uncertainties induced by the model parameters, the S -wave and D -wave amplitudes. Our

result for 15k event yields,

$$\begin{aligned}\sigma_{(\theta_{K_1}=15^\circ)} &= 1.3^\circ, & \sigma_{(\theta_{K_1}=30^\circ)} &= 1.4^\circ, \\ \sigma_{(\theta_{K_1}=45^\circ)} &= 1.3^\circ, & \sigma_{(\theta_{K_1}=60^\circ)} &= 2.6^\circ, & \sigma_{(\theta_{K_1}=75^\circ)} &= 8.2^\circ.\end{aligned}\quad (37)$$

The fitted mass and width are well within their uncertainties, i.e. (1.270 ± 0.006) GeV and (0.090 ± 0.013) GeV, respectively. This clearly shows the difficulty of determining the θ_{K_1} angle at a few degree precision above $\sim 45^\circ$. However, it is quite fair to say that the $\tau^- \rightarrow K_1^- \nu_\tau \rightarrow (K^- \omega) \nu_\tau \rightarrow (K^- \pi^+ \pi^- \pi^0) \nu_\tau$ decay has certainly an ability to discriminate the two solutions, $\theta_{K_1} \sim 30^\circ$ and $\theta_{K_1} \sim 60^\circ$, obtained by the other experiments.

Next, we study a possible systematic uncertainty caused by the $SU(3)$ breaking effect. We discuss this systematic effect separately here, since, as mentioned earlier, the existence of the $SU(3)$ effect is still debatable: more theoretical investigation is needed to clarify whether this effect must be taken into account or not. We estimate the $SU(3)$ breaking effect as follows. We perform a fit of the same 15k event sample by introducing non-zero δ_s and measure the shift of the θ_{K_1} value. In order to estimate the maximum effect, we vary δ_s maximally, i.e. $\delta_s = -6^\circ(+6^\circ)$. The obtained results are (mass and width are fitted simultaneously)

$$\begin{aligned}\Delta\theta_{K_1(\theta_{K_1}=15^\circ)} &= +3.8^\circ (-3.7^\circ), & \Delta\theta_{K_1(\theta_{K_1}=30^\circ)} &= +2.8^\circ (-2.8^\circ), \\ \Delta\theta_{K_1(\theta_{K_1}=45^\circ)} &= +1.4^\circ (-1.6^\circ), & \Delta\theta_{K_1(\theta_{K_1}=60^\circ)} &= +1.7^\circ (+4.7^\circ), \\ \Delta\theta_{K_1(\theta_{K_1}=75^\circ)} &= -7.7^\circ (-3.5^\circ).\end{aligned}\quad (38)$$

The results show that the positive (negative) δ_s leads to a positive (negative) shift of the mixing angle for $\theta_{K_1} \lesssim 45^\circ$, which is consistent to what we can observe in Fig. 1. And for this lower range of θ_{K_1} , the uncertainties from the unknown $SU(3)$ effect could exceed the statistical error. For 60° and 75° , the trend of the sign of the shift is not seen and this is probably due to the large statistical error which causes a fluctuation, that is, the statistical error dominates over the $SU(3)$ breaking effect in this range of θ_{K_1} . The bottom line is, even after taking into account the systematic error coming from the $SU(3)$ breaking effect, on top of the statistical error, this measurement can still eliminate one of the two solutions, $\theta_{K_1} \sim 30^\circ$ and $\theta_{K_1} \sim 60^\circ$, obtained by the other experiments.

5 Conclusions

In this article, we proposed to measure the $\tau^- \rightarrow K_1^- \nu_\tau \rightarrow (K^- \omega) \nu_\tau \rightarrow (K^- \pi^+ \pi^- \pi^0) \nu_\tau$ decay to determine the axial vector mixing angle θ_{K_1} . We first derived the $\tau^- \rightarrow K_1^- \nu_\tau \rightarrow (K^- \omega) \nu_\tau \rightarrow (K^- \pi^+ \pi^- \pi^0) \nu_\tau$ differential decay

rate formula in order to understand the θ_{K_1} dependence of the $K\pi\pi\pi$ spectrum. The theoretical formula for this five body differential decay rate is obtained for the first time in this article. Using the obtained result, we performed a sensitivity study for determining the θ_{K_1} angle by assuming the Belle (II) experiment environment. The $K\pi\pi\pi$ spectrum contains two K_1 resonances, $K_1(1270)$ and $K_1(1400)$. The contribution from $K_1(1400)$ diminishes as the θ_{K_1} value increases. As a result, for a larger values of θ_{K_1} , let's say above $\sim 45^\circ$, the $K_1(1400)$ resonance becomes nearly invisible, which makes it difficult to distinguish the spectrums with different values of θ_{K_1} in this range. More quantitatively, the expected statistical errors for 15k event are $\sigma_{\theta_{K_1}} = \{\pm 1.3^\circ, \pm 1.4^\circ, \pm 1.3^\circ, \pm 2.6^\circ, \pm 8.2^\circ\}$ for $\theta_{K_1} = \{15^\circ, 30^\circ, 45^\circ, 60^\circ, 75^\circ\}$. This amount of data will be very soon available at the Belle (II) experiment.

We also discussed a possible correction to this result due to the $SU(3)$ breaking effect, which is related to the production of K_{1b} (1P_1) state from the axial vector current. The existence of this contribution is not confirmed and we urge a theoretical progress on this matter. In order to evaluate its possible impact, we included the maximum of $\pm 10\%$ $SU(3)$ breaking effect. The result shows that it can shift the measurement of θ_{K_1} by $\Delta\theta_{K_1} = \{\pm 3.8^\circ, \pm 2.8^\circ, \pm 1.4^\circ\}$ for $\theta_{K_1} = \{15^\circ, 30^\circ, 45^\circ\}$. We find that the statistical error dominates in the case of the higher values of θ_{K_1} , i.e. $\theta_{K_1} = 60^\circ$ and 75° .

The other experiments found the θ_{K_1} angle to be $\sim 30^\circ$ or $\sim 60^\circ$ and to eliminate one of the solutions is a very important matter. For these values of θ_{K_1} , the $\tau^- \rightarrow K_1^- \nu_\tau \rightarrow (K^- \omega) \nu_\tau \rightarrow (K^- \pi^+ \pi^- \pi^0) \nu_\tau$ can determine θ_{K_1} at the precision of

$$\delta\theta_{K_1} = \pm 3.1^\circ \quad (\text{for } \theta_{K_1} = 30^\circ), \quad \delta\theta_{K_1} = \pm 5.4^\circ \quad (\text{for } \theta_{K_1} = 60^\circ)$$

where the statistical uncertainty with 15k event at Belle (II) and the systematic uncertainty from 10% $SU(3)$ breaking effect are added by quadrature. Therefore, we conclude that the $\tau^- \rightarrow K_1^- \nu_\tau \rightarrow (K^- \omega) \nu_\tau \rightarrow (K^- \pi^+ \pi^- \pi^0) \nu_\tau$ measurement can discriminate the two solutions for the θ_{K_1} angle obtained by the other experiments and determine it at this level of precision.

Acknowledgements This work was in part supported by the TYL-FJPPL (France-Japan Particle Physics Laboratory). We acknowledge the Belle collaboration for letting us to use the simulation software. E.K. would like to thank F. Le Diberder and B. Moussallam for valuable discussions.

Data Availability Statement This manuscript has no associated data or the data will not be deposited. [Authors' comment: This article includes only theoretical computation and simulation. It does not deal with any experimental data.]

Open Access This article is licensed under a Creative Commons Attribution 4.0 International License, which permits use, sharing, adaptation, distribution and reproduction in any medium or format, as long as you

give appropriate credit to the original author(s) and the source, provide a link to the Creative Commons licence, and indicate if changes were made. The images or other third party material in this article are included in the article's Creative Commons licence, unless indicated otherwise in a credit line to the material. If material is not included in the article's Creative Commons licence and your intended use is not permitted by statutory regulation or exceeds the permitted use, you will need to obtain permission directly from the copyright holder. To view a copy of this licence, visit <http://creativecommons.org/licenses/by/4.0/>.
Funded by SCOAP³.

References

1. W. Altmannshofer et al., The Belle II physics book. PTEP **2019**(12), 123C01 (2019). [Erratum: PTEP **2020**, 029201 (2020)]
2. E. Kou, A.L. Yaouanc, A. Tayduganov, Determining the photon polarization of the $b \rightarrow s\gamma$ using the $B \rightarrow K_1(1270)\gamma \rightarrow (K\pi\pi)\gamma$ decay. Phys. Rev. D **83**, 094007 (2011)
3. V. Bellée, P. Pais, A. Puig Navarro, F. Blanc, O. Schneider, K. Trabelsi, G. Veneziano, Using an amplitude analysis to measure the photon polarisation in $B \rightarrow K\pi\pi\gamma$ decays. Eur. Phys. J. C **79**(7), 622 (2019)
4. E. Kou, C.-D. Lü, Y. Fu-Sheng, Photon polarization in the $b \rightarrow s\gamma$ processes in the left-right symmetric model. JHEP **12**, 102 (2013)
5. W. Wang, Y. Fu-Sheng, Z.-X. Zhao, Novel method to reliably determine the photon helicity in $b \rightarrow s\gamma$. Phys. Rev. Lett. **125**(5), 051802 (2020)
6. N. Adolph, G. Hiller, A. Tayduganov, Testing the standard model with $D_{(s)} \rightarrow K_1(\rightarrow K\pi\pi)\gamma$ decays. Phys. Rev. D **99**(7), 075023 (2019)
7. Z.-R. Huang, M. Ali Paracha, I. Ahmed, C.-D. Lü, Testing leptoquark and Z' models via $B \rightarrow K_1(1270, 1400)\mu^+\mu^-$ decays. Phys. Rev. D **100**(5), 055038 (2019)
8. H.-Y. Cheng, K.-C. Yang, Hadronic charmless B decays $B \rightarrow AP$. Phys. Rev. D **76**, 114020 (2007)
9. H.-Y. Cheng, K.-C. Yang, Branching ratios and polarization in $B \rightarrow VV, VA, AA$ decays. Phys. Rev. D **78**, 094001 (2008) [Erratum: Phys. Rev. D **79**, 039903 (2009)]
10. J. Dalseno, Resolving the $\phi_2(\alpha)$ ambiguity in $B^0 \rightarrow a_1^\pm\pi^\mp$. JHEP **10**, 191 (2019)
11. M. Suzuki, Strange axial-vector mesons. Phys. Rev. D **47**, 1252–1255 (1993)
12. L. Burakovsky, J. Terrance Goldman, Constraint on axial-vector meson mixing angle from nonrelativistic constituent quark model. Phys. Rev. D **56**, 1368–1372 (1997)
13. D.-M. Li, B. Ma, Y. Hong, Regarding the axial-vector mesons. Eur. Phys. J. A **26**, 141–145 (2005)
14. A. Tayduganov, E. Kou, A. Le Yaouanc, The strong decays of K_1 resonances. Phys. Rev. D **85**, 074011 (2012)
15. H.-Y. Cheng, Revisiting axial-vector meson mixing. Phys. Lett. B **707**, 116–120 (2012)
16. H.-Y. Cheng, Mixing angle of K_1 axial vector mesons. PoS Hadron **2013**, 090 (2013)
17. D. Buskulic et al., A study of tau decays involving eta and omega mesons. Z. Phys. C **74**, 263–273 (1997)
18. R. Barate et al., Study of tau decays involving kaons, spectral functions and determination of the strange quark mass. Eur. Phys. J. C **11**, 599–618 (1999)
19. K.E. Arms et al., Study of tau decays to four-hadron final states with kaons. Phys. Rev. Lett. **94**, 241802 (2005)
20. A. Tayduganov, Electroweak radiative B-decays as a test of the Standard Model and beyond. PhD thesis, Orsay (2011)
21. H.J. Lipkin, Implications of tau decays into strange scalar and axial vector mesons. Phys. Lett. B **303**, 119–124 (1993)
22. S. Jadach, B.F.L. Ward, Z. Was, The precision Monte Carlo event generator K K for two fermion final states in e^+e^- collisions. Comput. Phys. Commun. **130**, 260–325 (2000)
23. S. Jadach, B.F.L. Ward, Z. Was, Coherent exclusive exponentiation for precision Monte Carlo calculations. Phys. Rev. D **63**, 113009 (2001)
24. S. Jadach, J.H. Kuhn, Z. Was, TAUOLA: a library of Monte Carlo programs to simulate decays of polarized tau leptons. Comput. Phys. Commun. **64**, 275–299 (1990)
25. M. Jezabek, Z. Was, S. Jadach, J.H. Kuhn, The tau decay library TAUOLA, update with exact $O(\alpha)$ QED corrections in $\tau \rightarrow \mu(e)\nu\bar{\nu}$ decay modes. Comput. Phys. Commun. **70**, 69–76 (1992)
26. S. Jadach, Z. Was, R. Decker, J.H. Kuhn, The tau decay library TAUOLA: version 2.4. Comput. Phys. Commun. **76**, 361–380 (1993)
27. E. Kou, K. Hayasaka, F. Le Diberder, In preparation
28. C. Daum et al., Diffractive production of strange mesons at 63-GeV. Nucl. Phys. B **187**, 1–41 (1981)